The Electrochemical Characterisation of Graphite Felts

Supporting Information

Robert E. G. Smith,[a] Trevor J. Davies,[b, c] * Nicholas de B. Baynes,[c] and Richard J. Nichols.[a]

a. Department of Chemistry, University of Liverpool, Crown Street, Liverpool, UK, L69 7ZD.

b. Department of Natural Sciences, University of Chester, Thornton Science Park, Ince, UK, CH2 4NU.

c. ACAL Energy Limited, The Heath Business and Technical Park, Cheshire, UK, WA7 4QX

*Author to whom all correspondence should be addressed

Email: t.davies@chester.ac.uk

Tel.: +44 (0)1244 512297

1. Experimental

1.1 Solution resistance compensation

Figure S1(a) illustrates cyclic voltammograms recorded at 0.1 V s^{-1} with a GF electrode in 0.1 mM ferrocene/0.1 M TBAP. The dashed curve corresponds to the uncompensated cyclic voltammogram whereas the solid curve is the voltammogram with 85 % compensation of solution resistance. The measured solution resistance in the cell was 15 Ohm. The magnitude of the current signal is ~10 mA, producing an "*IR* drop" value of ~150 mV (where *I* is the current and *R* is the solution resistance). This is large enough to distort the signal, which is illustrated by the difference between the compensated and uncompensated voltammograms in Figure S1(a). An alternative to electronically compensating for solution resistance is to reduce the concentration of the redox system, thus reducing the magnitude of the current and associated "*IR* drop". This is illustrated in figure S1(b) where applying electronic *IR* compensation for solution resistance had little to no effect for the 10 µM ferrocene solution which is ten times more dilute that in Figure S1(a) Both IR compensation and redox species dilution were used to obtain voltammograms suitable for data analysis.

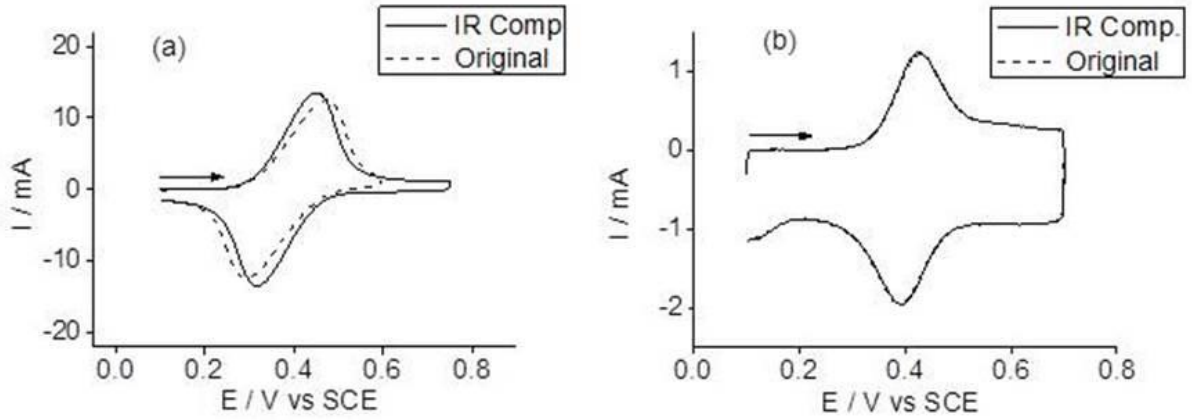

Figure S1. Cyclic voltammetry of a GF electrode in (a) 0.1 mM and (b) 10 µM ferrocene solution, before and after automatic solution resistance compensation. Scan rate = 0.1 V s^{-1}

1.2 Simulations

Figure S2 illustrates plots of peak cathodic current, I_p^c, vs. scan rate, v, and I_p^c vs. $v^{0.5}$ for the porous electrode discussed in Section 3 of the main text. At low scan rates the peak current is proportional to scan rate, indicative of thin layer voltammetry and finite diffusion, whereas at high scan rates the peak current is proportional to the square root of scan rate, indicative of semi-infinite diffusion.

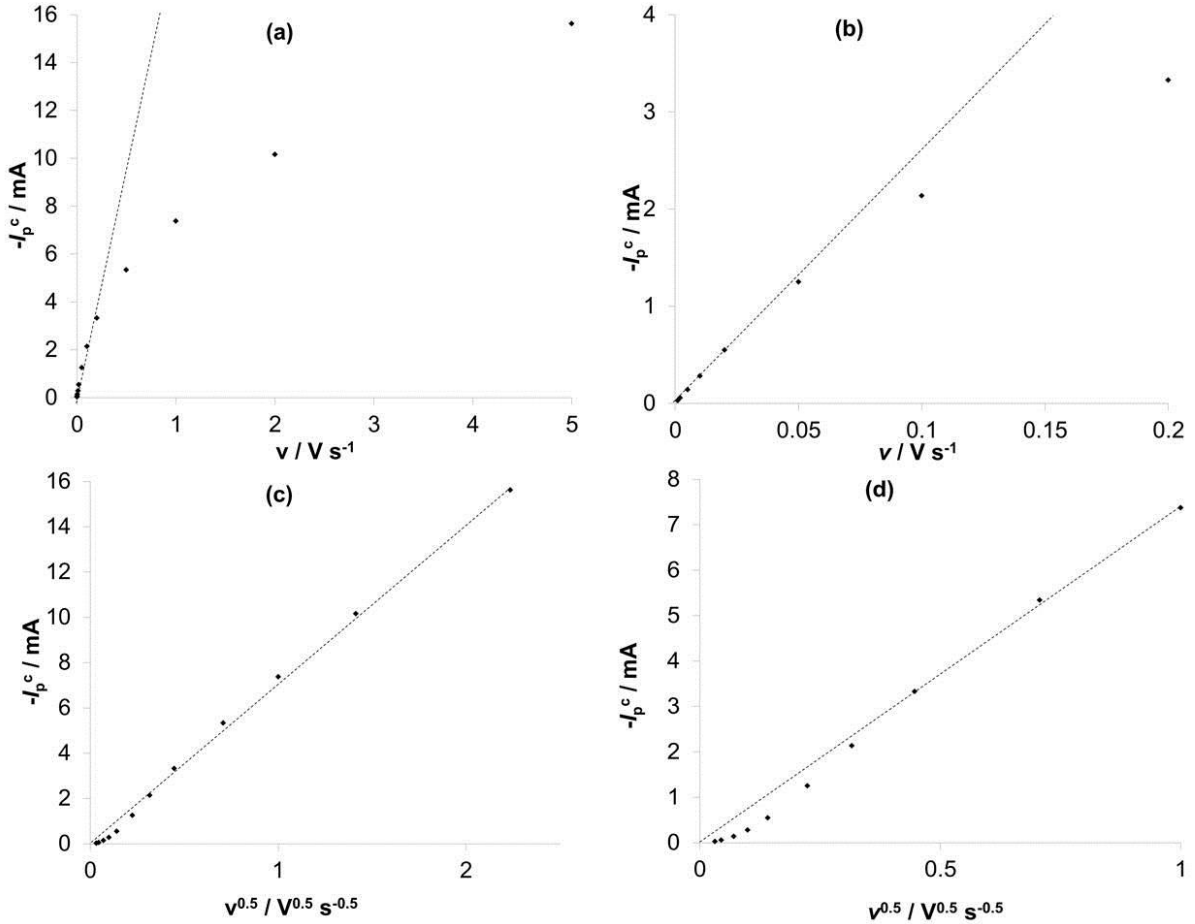

Figure S2. (a) Cathodic peak current vs. scan rate for the porous electrode of total area 10 cm^2 and average pore radius of 30 µm. (b) Magnification of the linear region in (a). (c) Cathodic peak current vs. square root of scan rate for the porous electrode of total area 10 cm^2 and average pore radius of 30 µm. (d) Magnification of the non-linear region in (c).

2. Results and Discussion

2.1 Ferricyanide Voltammetry

Figure S3(a-d) illustrates plots of peak cathodic current, I_p^c, vs. scan rate, v, and I_p^c vs. $v^{0.5}$ for a GF electrode in 0.1 mM ferricyanide solution. The results are very similar to the simulated plots in Figure 6 of the main document, and indicate a transition from finite diffusion/thin layer voltammetry at low scan rates to semi-infinite diffusion at high scan rates. The amount of diffusion layer overlap inside the porous electrode changes with scan rate, which suggests the simulation method proposed in the previous section can be used in combination with these experimental results to simultaneously determine the total (smooth) surface area and average pore size for this GF electrode.

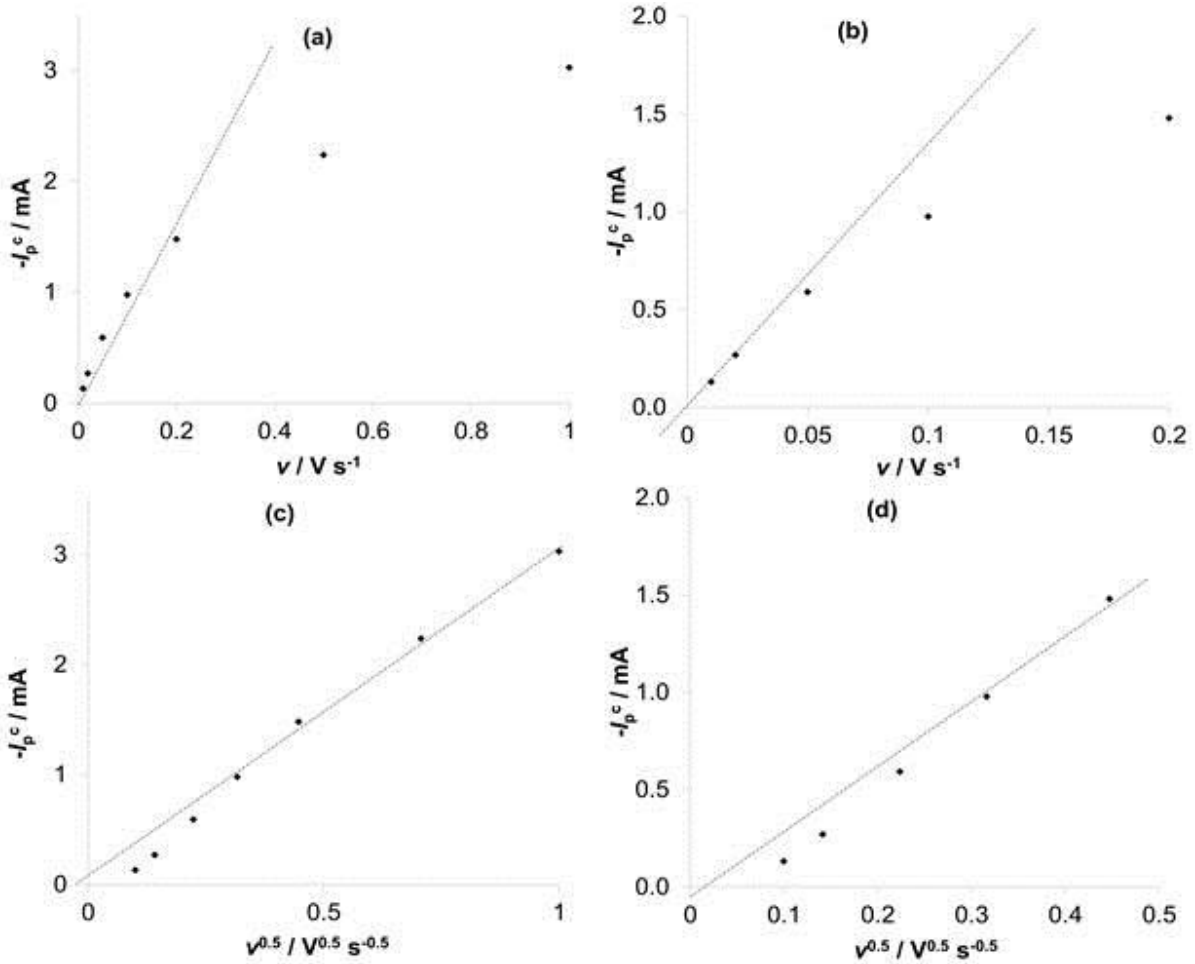

Figure S3. (a) Cathodic peak current vs. scan rate for a GF electrode in 0.1 mM ferricyanide solution. (b) Magnification of the linear region in (a). (c) Cathodic peak current vs. square root of scan rate for a GF electrode in 0.1 mM ferricyanide solution. (d) Magnification of the non-linear region in (c).

2.2 Ferrocyanide Voltammetry

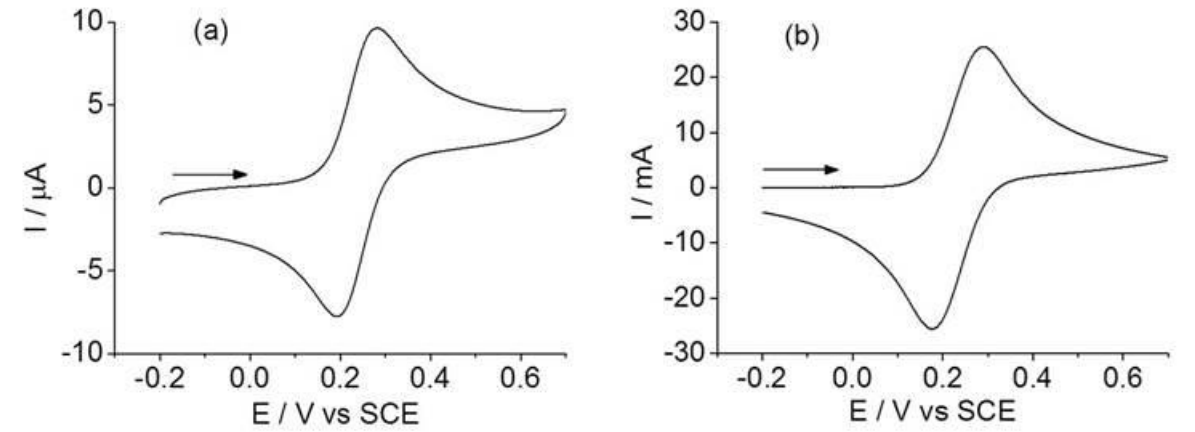

Figure S4. Cyclic voltammetry of (a) an EPPG and (b) a GF electrode in 1.0 mM ferrocyanide/1.0 M KCl(aq.) solution. Scan rate = 0.05 V s^{-1}.

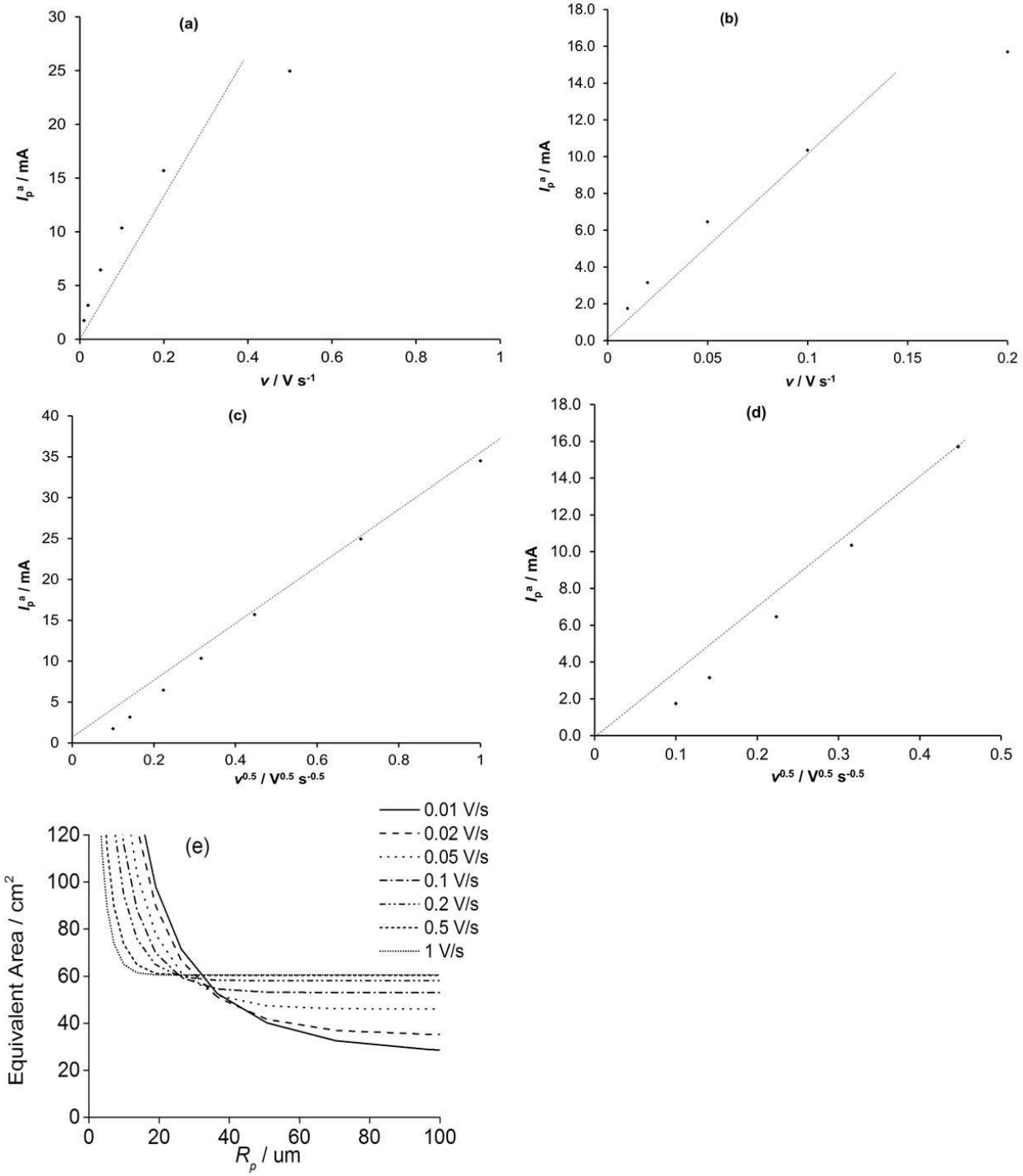

Figure S5. (a) Anodic peak current vs. scan rate for a GF electrode in 0.1 mM ferrocyanide solution. (b) Magnification of the linear region in (a). (c) Anodic peak current vs. square root of scan rate for a GF electrode in 0.1 mM ferrocyanide solution. (d) Magnification of the non-linear region in (c). (e) Simulated curves of equivalent surface area vs. pore radius using the anodic peak current results from a GF electrode in a 1.0 mM ferrocyanide solution.

In addition to the ferricyanide, the ferrocyanide redox system was also investigated with GF electrodes. However as a higher concentration was used it was necessary to apply solution resistance compensation. For the GF electrode in 1.0 mM ferrocyanide solution, Figure S4(b), 85% of the measured 6.6 Ohm solution resistance was compensated for. The ferrocyanide system is in excellent agreement with the ferricyanide system in terms of both voltammetric characteristics and the deduced felt properties (e.g. pore radius and surface area) in Table 2. The same relationship

between scan rate, the square root of scan rate and peak anodic current, as shown previously, Figure S3(a-d), is also seen for ferrocyanide Figure S5(a-d).

The equivalent area vs. R_p plot shown in Figure S5(e) is comparable to both the initial simulated plot and that of ferricyanide (Figures 7 and 9 of the main document). However, the crossover region is more diffuse than previously. Whilst this produces a larger range for both pore size and equivalent area, the low scan rate results are more likely to have the largest error due to the issues discussed in the previous section. The higher scan rate results suggest values of R_p = 30 µm and area = 60 cm^2. This agrees well with the theoretical surface area given in Table 2 of the main document.

2.3 Vanadium(V) Voltammetry

Vanadium redox flow batteries (VRFBs) are of ever increasing industrial and academic interest. With the growing global demand for long lasting, stable energy storage systems the VRFB has been extensively studied and is widely discussed in literature [1]. A large amount of research on this system has used either flow cell or rotating disc experiments. Whilst these techniques provide a host of useful information, especially regarding the systems use within flow batteries, they can be both difficult to set up and costly in terms of both expenditure and time. By following the techniques set out in this paper, the vanadium(V) oxide system can be studied effectively, even at minute concentrations and with very little effort. This makes rapid screening of electrode modifications possible and could significantly enhance up the development of more efficient VRFBs.

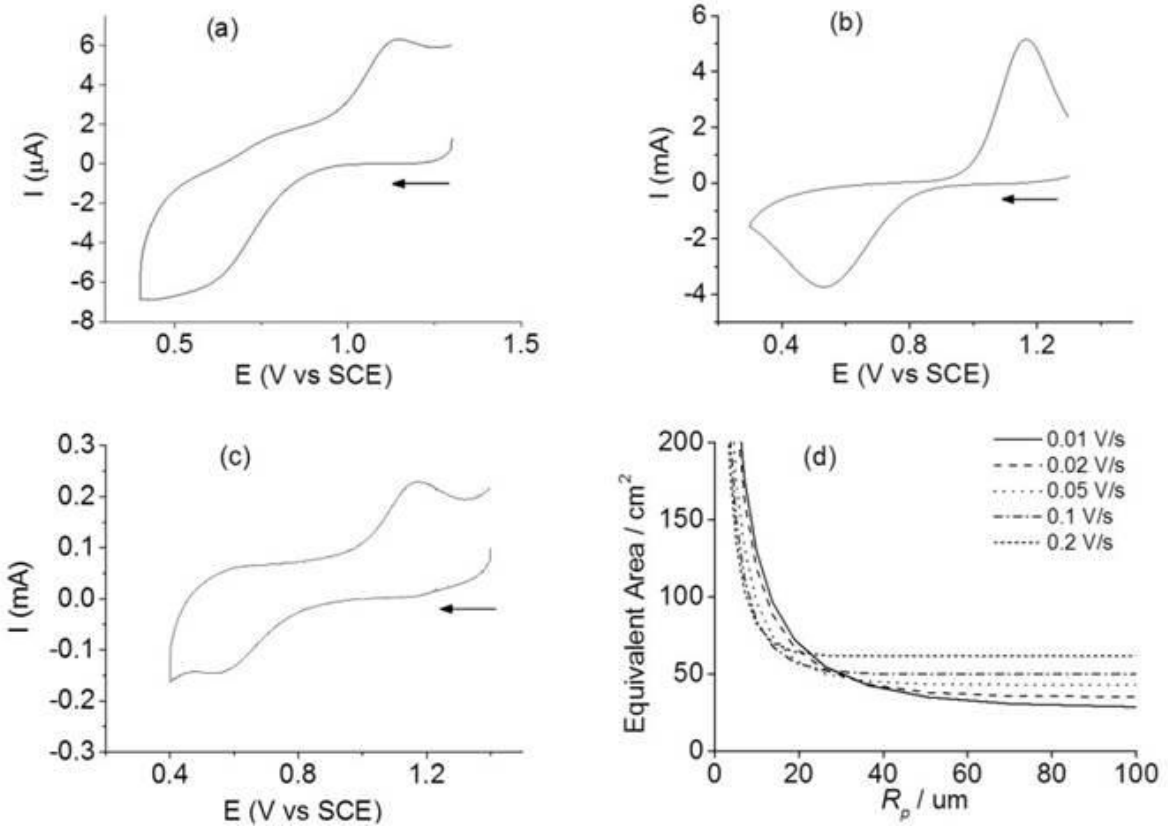

Figure S6. Cyclic voltammetry of (a) EEPG electrode, (b) GF electrode in 1.6 mM vanadium(V) / 4 M H_2SO_4(aq.) solution and (c) GF electrode in 32 µM vanadium(V) / 4 M H_2SO_4(aq.) solution. Scan rate = 0.05 V s^{-1}. (d) Simulated curves of equivalent surface area vs. pore radius using the cathodic peak current results from a GF electrode in a 1.6 mM vanadium(V) solution.

A solution of 1.6 mM vanadium(V) in 4 M H_2SO_4(aq.) was produced and investigated using the above voltammetric method. Again values for both *D* and *k* were determined from cyclic voltammetry using the standard 3 mm diameter carbon electrodes, Table 1 (in the main text), and these compare well with literature values [2]. The difficulties in measuring this system with standard carbon electrodes, such as the poor peak definition shown in Figure S6(a), give an excellent opportunity to showcase the ability of the GF electrodes. Figure S6(a) shows the cyclic voltammogram for 1.6 mM vanadium(V) with a PFC working electrode at 50 mV s^{-1}. In comparison Figure 14(b) shows the cyclic voltammogram for the same solution but with a GF electrode. The GF is clearly superior at both resolving the redox peaks and improving the profile of the voltammogram. The GF felt was also able to distinguish the redox peaks of a 32 µM solution of the vanadium(V), shown in Figure S6(c). It was not possible to distinguish these redox peaks with the 3 carbon disc electrodes at this low concentration. Given the challenging nature of this redox system, the ability of the GF electrode to distinguish peaks at such minute concentrations is particularly impressive.

The equivalent surface area vs. R_p plot for the 1.6 mM vanadium system is shown in Figure S6(d). The range of equivalent surface area and pore sizes are much greater than for the previous redox systems. Despite this they still compare well to the predicted values, shown in Table 2 of the main document, as well as the two previous systems.

2.3 Ferrocene Voltammetry

To further examine the ability of the GF electrodes, a non-aqueous redox system was also investigated. A solution of 0.1 mM ferrocene in 0.1 M TBAP/acetonitrile was used for the standard carbon disc electrodes, whereas 10 µM ferrocene in 0.1 M TBAP/acetonitrile was used for the GF samples. The non-aqueous nature of the ferrocene solution eliminated the wettability issue of the GF and therefore removed the requirement for the ethanol pre-treatment step. Values of *D* and k^e were again determined using the traditional carbon disc electrodes, Table 1 (in the main text), and are within the range of previous literature values [3]. Figure S7 shows a comparison between the EPPG and GF electrodes in the ferrocene solution.

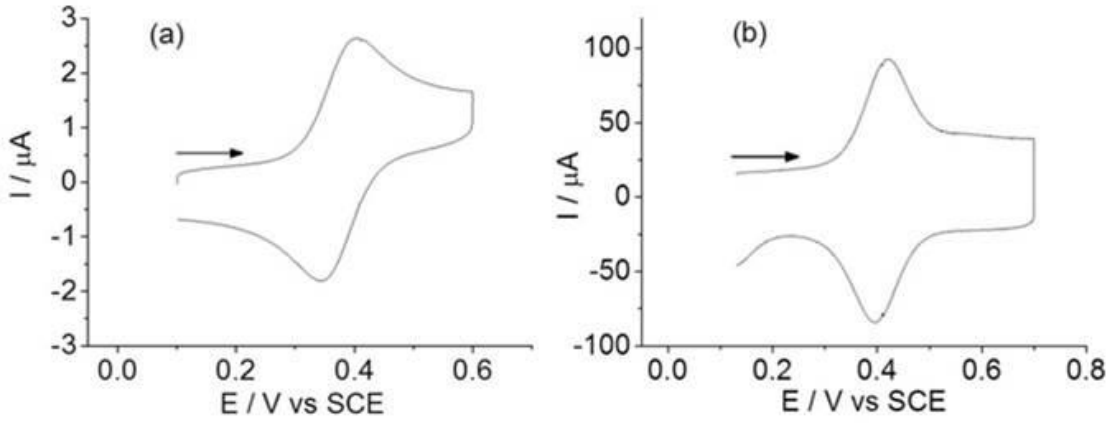

Figure S7. Cyclic voltammetry of (a) an EPPG electrode in 0.1 mM ferrocene solution and (b) a GF electrode in 10 µM ferrocene solution. Scan rate = 0.05 V s^{-1}.

The results for GF electrodes in ferrocene/acetonitrile solution follow the same trends seen in the previous aqueous systems, as shown in Figure S8(a-d). The equivalent area vs. average pore radius plot determined using the simulation method is shown for one of the GF electrodes in the ferrocene/acetonitrile system in Figure S8(d). As observed, the cross over region is much more diffuse for this system compared to the aqueous systems. The cause could be the higher diffusion coefficient of ferrocene in acetonitrile, making the lower scan rate results even more prone to the simulation error discussed in the previous section. Discarding the 0.01 and 0.02 V s^{-1} data, the results agree well with the other systems.

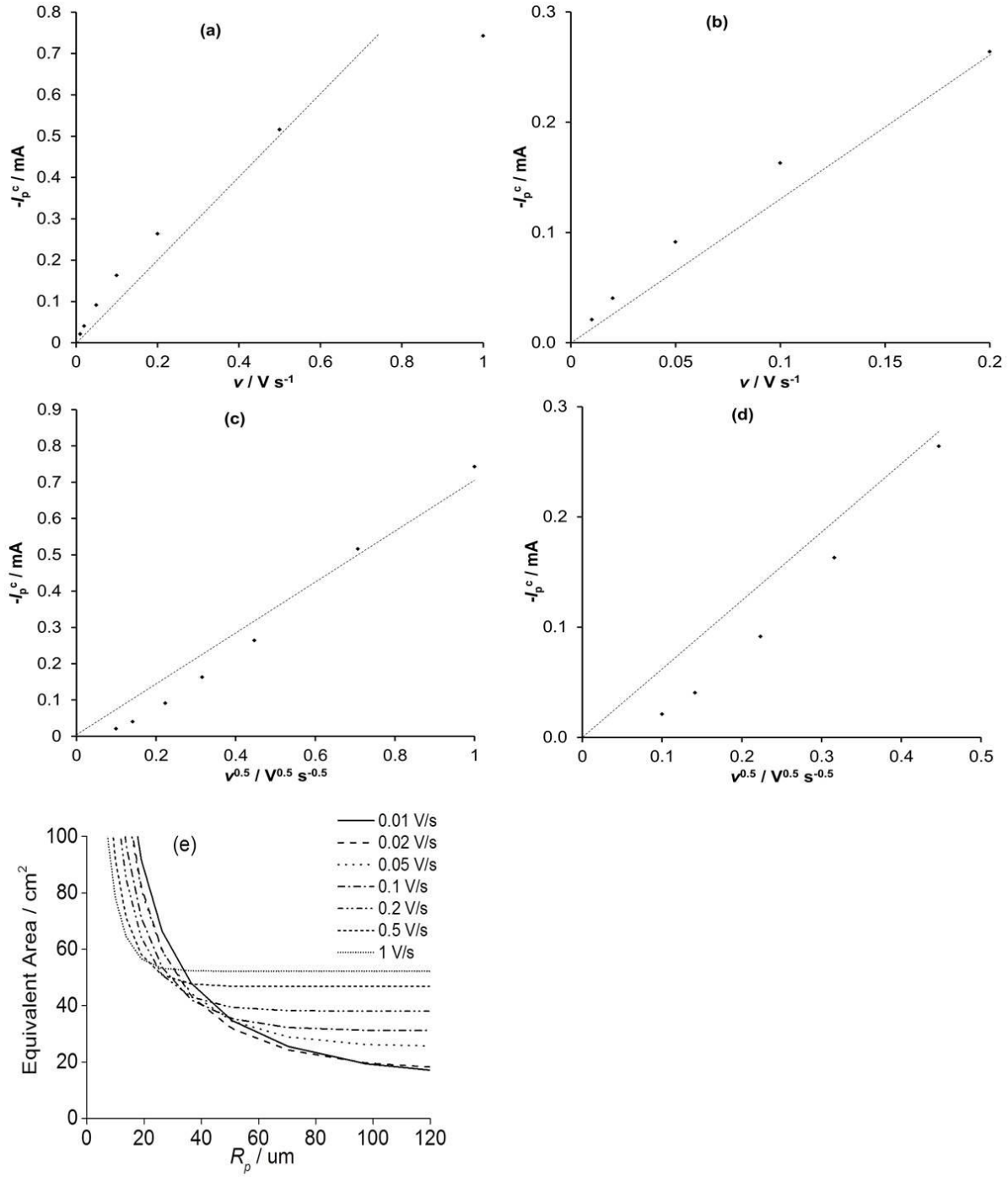

Figure S8. (a) Anodic peak current vs. scan rate for a GF electrode in 10 µM ferrocene solution. (b) Magnification of the linear region in (a). (c) Anodic peak current vs. square root of scan rate for a GF electrode in 10 µM ferrocene solution. (d) Magnification of the non-linear region in (c). (e) Simulated curves of equivalent surface area vs. pore radius using the anodic peak current results from a GF electrode in a 10 µM ferrocene solution.

2.4 Fibre Surface Structure

The capacitance of an electrode surface can be determined via cyclic voltammetry within a potential window where no faradaic reactions occur. Figure S9 illustrates an example of the capacitance scans recorded in the ferrocene systems. These are typical results with the capacitive current, *I*, increasing linearly with scan rate, ν. For these voltammograms the capacitance, *C*, of the surface can be calculated using equation 1;

$$I = C\nu \qquad (1)$$

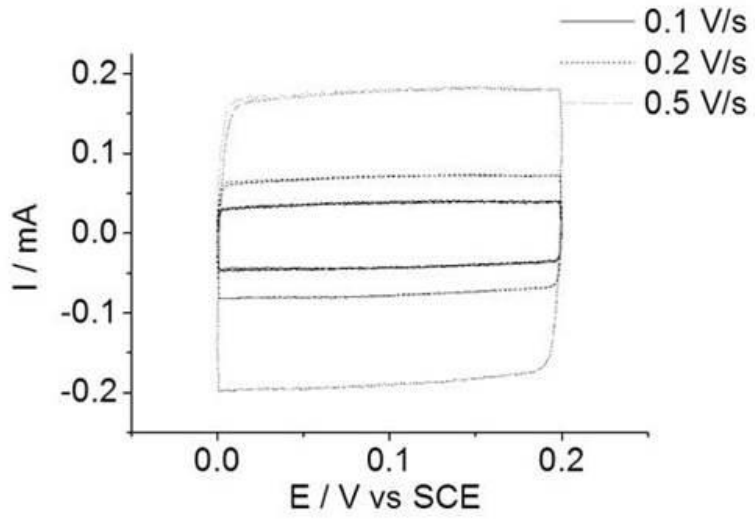

Figure S9. Capacitance measurements using cyclic voltammetry of GF in 10 μM ferrocene solution at the shown scan rates.

References

[1] G. Kear, A. Shah, F. C. Walsh, Int. J. Energy Res. 36 (2012) 1105-1120.

[2] L. Hui-jun, X. Qian, Y. Chuan-wei, C. Ya-zhe, Q. Yong-lian, Int. J. Electrochem. Sci. 6 (2011) 3483-3469

[3] Y. Wang, E. I. Rogers, R. G. Compton, J. Electroanal. Chem. 648 (2010) 15-19.